NASA Technical Memorandum 100853

Ray Tracing Optical Analysis of Offset Solar Collector for Space Station Solar Dynamic System

Kent S. Jefferies
Lewis Research Center
Cleveland, Ohio

Prepared for the
23rd Intersociety Energy Conversion Engineering Conference
cosponsored by the ASME, AIAA, ANS, SAE, IEEE, ACS, and AIChE
Denver, Colorado, July 31—August 5, 1988

NASA

RAY TRACING OPTICAL ANALYSIS OF OFFSET SOLAR COLLECTOR FOR SPACE STATION SOLAR DYNAMIC SYSTEM

Kent S. Jefferies
National Aeronautics and Space Administration
Lewis Research Center
Cleveland, Ohio 44135

SUMMARY

OFFSET, a detailed ray tracing computer code, was developed at NASA Lewis Research Center to model the offset solar collector for the Space Station solar dynamic electric power system. This model traces rays from 50 points on the face of the Sun to 10 points on each of 456 collector facets. The triangular facets are modeled with spherical, parabolic, or toroidal reflective surface contour and surface slope errors. The rays are then traced through the receiver aperture to the walls of the receiver. Images of the collector and of the Sun within the receiver produced by this code provide insight into the collector receiver interface. Flux distribution on the receiver walls, plotted by this code, is improved by a combination of changes to aperture location and receiver tilt angle. Power loss by spillage at the receiver aperture is computed and is considerably reduced by using toroidal facets.

E-4056-1

INTRODUCTION

A Brayton cycle solar dynamic electric power system is being developed for a possible future enhancement of the Space Station's capabilities. The solar dynamic system uses a parabolic collector to reflect solar energy into a cylindrical receiver cavity. This solar energy heats a gas which rotates a turbogenerator that produces electric power. The current design uses an offset collector configuration which is one in which the parabolic vertex, instead of being located at the center of the collector, is offset to a point near the outer edge of the collector. To successfully develop the power system, it is necessary to understand the flux distributions within the receiver cavity produced by reflections from the offset collector. A ray tracing computer code is being developed at the NASA Lewis to evaluate intensity and distribution of the collected solar flux on the inside walls of the receiver.

In addition to the optical analysis of the offset collector being done at NASA Lewis, optical analysis of this collector has also been performed by Georgia Tech Research Institute, GTRI, using their OPTIC code (ref. 1), by McDonnell Douglas Astronautics Company, MDAC, using their DPAP (Dish Performance Analysis Program) code (ref. 2), and by Harris Corporation. The NASA Lewis analysis is intended for developing an understanding of the collector-receiver interface for guiding the contracted efforts. GTRI developed OPTIC to support experimental testing of receivers for terrestrial solar dynamic systems. OPTIC has been validated by direct comparison to experimental output. GTRI used OPTIC in providing analytical support to space station power system

contractor, Rocketdyne, and to the subcontractor for collector development, Harris, in developing a preliminary collector design. Harris has used their code for designing the collector and for manufacturing an advanced development version of the collector. MDAC's DPAP code was written to support development of terrestrial solar dynamic power systems and has been validated by direct comparison with experimental output. MDAC modified their DPAP code to simulate the offset collector in order to develop an optical measuring system for testing the offset collector.

OFFSET COLLECTOR AND RECEIVER GEOMETRY

The geometry of the offset solar collector and receiver is shown in figure 1. Note that the 19 hexagonal collector panels are all to one side of the axis of the parent paraboloid. This configuration eliminates blockage of the collector by the receiver. It also enables mounting of the collector and receiver directly to the transverse boom of the Space Station and thereby reduces the moment of inertia of the solar dynamic power system. The receiver is positioned at the focal point of the parabola. The receiver is cylindrical in shape with a small opening (aperture) at one end to receive the solar rays. For a symmetric concentrator configuration, the receiver would have been positioned with its axis along the axis of the parabola. However, with an offset paraboloid, the receiver is tilted so that its axis points approximately toward the center of the offset collector.

Collector Facets

The solar collectors for the Space Station are ~17 m in diameter. Each collector will be subdivided into 19 hexagonal panels about 4 m in diameter that can fit crosswise in the Space Shuttle. These hexagonal panels will each be subdivided into 24 triangular facets which are ~1 m on a side. This size is easier to manufacture and by staggering the facets, the panel thickness and therefore the packaging volume can be reduced by one-third.

An advanced development collector is currently being fabricated with spherical approximations to the parabolic shape and contour. The 4 m hexagonal panels are mapped to the surface of a sphere which closely approximates the shape of the paraboloid. This enables equal spacing between the panels and thereby simplifies collector design. The individual triangular facets also are manufactured with a spherical contour. Four radii of curvature are used for the spherical facets to approximate the parabolic contour in different regions of the collector. The radii in different regions are shown in figure 2.

Receiver

The receiver shown in figure 3 has a cylindrical sidewall, circular backwall, and circular aperture plate. The aperture plate has a small aperture centered on it to admit reflected solar rays. This receiver for the space station solar dynamic system has 82 working fluid tubes surrounded by donuts of phase change material for thermal energy storage.

COMPUTER CODE

This section describes certain unique or important features of the OFFSET code. The equations for selecting representative solar rays are of particular significance because they have potential applications for selecting representative samples, for spacing items and for locating computer code nodes. Options built into the code for selecting spherical, parabolic, or toroidal facet contour and for determining facet orientation are discussed. There is also a discussion of how specularity and surface slope error of the reflective surface are represented.

Representative Solar Rays

Equations were developed to choose ray originating locations on the Sun representative of the size and brightness distribution of the Sun. The following two equations generate a pseudorandom distribution of 50 points on a unit circle that are evenly distributed. This distribution avoids both the clustering that occurs with truly random points and the linear patterns of points on a grid.

$$\text{Radius}(I) = \sqrt{.01 \times (2I - 1)} \tag{1}$$

$$\text{Angle}(I) = 0.84\pi I \tag{2}$$

The exact value of the constant, 0.84π, is the key to achieving this random pattern. For example, a value of 0.8π would cause all the points to line up on five straight lines.

The center of the Sun is about 50 percent brighter than the edge of the Sun. This brightness variation, commonly called solar limb darkening, is due primarily to the fact that the Sun consists of layers of radiating gases. The following equation was used instead of equation (1) to select solar ray originating locations, shown in figure 4, that are representative of a limb darkened Sun.

$$\text{Radius}(I) = \sqrt{.00845(2I - 1) + 0.155\ \text{Radius}(I)^{4.4}} \tag{3}$$

Equations (1) and (3) differ in that equation (1) chooses the radii so that 2 percent of the area is between two consecutive radii and equation (3) chooses radii so that 2 percent of the solar radiation is between them. Other formulas for Radius(I) could be developed to produce the desired radial spacings for other applications.

Facet Contour and Orientation

Choices are built into the computer code for modeling the current design and possible advanced designs. The facet contours can be chosen to be segments of paraboloids, to be spherical or to be toroidal. Different radii of curvature can be chosen for different groups of facets to better approximate the paraboloid. Facet alignment can either be specified by the locations of the corners of the facets or by choosing ideal alignment such that the central ray from the Sun reflected from the center of the facet will intersect the center of the receiver aperture. The center of curvature is calculated based on the

alignment of the facet and is used to compute the normal direction at points on each spherical or toroidal facet. Alternatively, if paraboloidal contours are chosen, the normal direction at each point is chosen so that that point will reflect the central ray to the center of the aperture.

Specularity and Slope Error

Facets will have deviations from the design contour, called surface slope error, and local imperfections which reduce the sharpness of the reflected image, called specular error. Surface slope errors are introduced during the manufacturing process and subsequent handling of the facet. Specular error is due to the molecular structure of the reflective surface material and its method of application. Specularity is measured by the angular spreading of the reflected light. In the computer code, the angular distribution of the solar ray originating locations, shown in figure 4, is vectorially added to a normal distribution of specular angle to determine the angular distribution of the reflected sunlight. This angular distribution is then approximated by 50 representative reflected rays. The same distribution of reflected rays relative to the surface normal is used at every point on the collector. Surface slope errors are random deviations from the design surface contour. Radial and tangential components of surface slope error are computed for each nodal point using a random number generator and the following equations to generate normal distributions.

$$\text{Radial} = \sigma\sqrt{-2\ \ln(r_1)\ \sin(2\pi\ r_2)} \tag{4}$$

$$\text{Tang'l} = \sigma\sqrt{-2\ \ln(r_1)\ \cos(2\pi\ r_2)} \tag{5}$$

where r_1 and r_2 are random numbers chosen independently for each nodal point and σ is the standard deviation of the slope error.

Nodal Points on Each Facet

The computer code provides for two possible arrangements, shown on figure 5, of nodal points on the triangular facets. The arrangement of nodal points along the edges of the facets, as shown on figure 5(a), enables plotting of facet outlines. The alternate arrangement of nodal points at the centers of nine subtriangles, as shown on figure 5(b), enables a more accurate computation of flux profiles. There is a tenth point at the center of the facet which is used for reference purposes, but does not enter into the computation of flux profiles.

COMPUTED IMAGES WITHIN THE RECEIVER

Computed light patterns within the receiver for certain cases show the effect of different elements of the code. The Sun, represented by 50 rays, strikes a single point on the collector and produces an image of the Sun inside the receiver. Different images are produced when different points on the collector are considered. Alternatively, rays from a single point on the Sun strike all of the points on the collector and produce an image of the collector, i.e., images of its facets within the receiver. These images will change

when different assumptions are made about the facet contours and their surface slope error.

Images of the Sun

Rays from the Sun striking a single point on the collector will be reflected into the receiver and form an image of the Sun inside the receiver. A flattened view of the cylindrical receiver is shown in figure 6. Ideal images of the 19 hexagonal panels within the receiver are shown for reference. Images of the Sun formed by 50 light rays reflected from the center of each of the 19 hexagonal panels are also shown on this receiver diagram. Note that the size of the solar images varies by about a factor of three. The size of these images is determined primarily by the angles of intersection of the rays with the receiver walls and by the distance from the centers of the panels to the receiver walls. The images of the Sun from the centers of the 12 outer panels are in an irregular column slightly to the left (aperture side) of the center of the cylindrical wall. The solar image from the central hexagon is close to the center of the backwall. The image in the center of the aperture is a focused solar image from all 19 panel center points.

Images of the Collector

Rays from a single point on the Sun striking the edges of the triangular facets form an image of the collector inside the receiver. The image shown in figure 7 was produced by assuming rays from the center of the Sun were reflected by parabolic facets with zero surface slope error. The focused image of the center point of the Sun is the single point at the center of the aperture. Note that the left edge of the pattern images the outer edge of the collector. The outer hexagonal panels whose images are furthest to the left are closest to the vertex of the parabola. Images of facets furthest from the vertex begin further to the right because the collector is offset rather than symmetric. The nodal points used for computing flux profiles are shown on one facet of each hexagonal panel in figure 7. These points are in the same positions relative to the facet images in figure 7 as they are relative to the facet in figure 5(b).

Slope Error and Spherical Contour

The effect of surface slope error on the nodal points of parabolic contoured facets is shown in figure 8. The radial and tangential components of surface slope error at each of these points are randomly selected from a Gaussian distribution with a standard deviation of 1 mrad. Note that 1 mrad of surface slope error moves the images of the nodal points to new locations relative to the ideal facet images. In some cases the images of the nodal points fall outside the triangular outlines of the ideal parabolic facet images.

Images of the selected spherically contoured facets produced by central solar rays are shown in figure 9. The facet images in figure 9 use the spherical radii of curvature chosen for the advanced development concentrator, but have no surface slope error. There are four different radii of curvature used for four groups of facets based on their distance from the vertex of the parabola. Note that the images have more size variation and some triangles are more

elongated than the images produced by ideal parabolic facets that were shown in figure 7. This is due primarily to astigmatism introduced by using spherical approximations to the ideal parabola. Also shown in figure 9 are nodal points from spherical facets with 1 mrad of random surface slope error. Some of these nodal points fall outside of the triangular outlines due to the random slope error.

RESULTS

The results of various analyses using the OFFSET code are described in the following sections. They include comparisons to DPAP and OPTIC computer code output, an improvement in receiver flux distribution by offsetting the receiver aperture from the axis of the cylindrical receiver, and improved aperture efficiency using toroidal facet contour.

DPAP and OPTIC Comparisons to OFFSET Results

MDAC's DPAP code output matches experimental measurements of aperture plane flux profile from solar collectors which MDAC has tested. MDAC modified DPAP to represent the offset collector in order to develop an optical measurement system for our use. Results from this simulation are presented in the form of aperture plane flux maps. The curves shown in figure 10 labeled MDAC show aperture flux versus radius derived from these maps. Also shown in figure 10 are curves of aperture flux versus radius from OFFSET. There is excellent agreement of this data both for the ideal spherical facets with zero slope error and for spherical facets with 3 mrad slope error.

The available results from GTRI's OPTIC code show receiver cylindrical side wall flux distribution for a previous configuration which only used 17 hexagonal panels instead of the current 19. This configuration is shown in figure 11. The OFFSET code was modified to approximate this configuration. Contour plots representing flux distribution on the receiver walls produced by OPTIC and OFFSET for this configuration are shown in figure 12. The plots are in good agreement for both the location and magnitude of the flux on the receiver walls.

Offset Receiver Aperture Improves Flux Distribution

A map of flux on the walls of the receiver for the 19 hexagonal panel collector design is shown in figure 13. Comparison of this figure to figure 12(a) with 17 hexagonal panels shows that these panels fill in the two low flux regions in the receiver flux map and give a more continuous flux distribution. There remains however an S-shape to the border of the low flux region on the aperture side of the receiver flux map. This S-shape is an image of the outer circumference of the collector distorted because the collector is an offset parabola. In an attempt to correct the S-shape of the flux profile, the receiver was repositioned so that the focal point of the parabola was near the edge of the circular receiver aperture plate. This configuration is shown in figure 14. The focal point, which in figure 1 had been on the receiver axis is near the edge of the aperture plate. The receiver aperture would be "offset" from the receiver axis to this new relative location of the focal point near

the edge of the aperture plate. The receiver tilt angle between the optical axis of the parabola and the receiver axis is increased. The resulting flux map in figure 15 shows a straighter shape to the border of the low flux region on the aperture side of the receiver wall. An additional and unexpected major benefit of this configuration change is that the region near the aperture that does not see solar flux is about one-third smaller than for the previous configuration. This may increase the effectiveness of the receiver tubes and their thermal energy storage and thereby enable some reduction in the receiver size.

Toroidal Facets

Toroidal facets can better approximate the complex contour of a parabola than spherical facets because they have different radii of curvature in two orthogonal directions. This is especially important for the Space Station offset collector, because it has an f/D ratio of 0.35, which causes considerable astigmatism. However, toroidal facets need to be oriented so that the longest radius of curvature of the toroid is in the same direction as the longest radius of curvature of the paraboloid. This direction is along the parabolic arc and is radially outward from the axis of the parabola. To orient the facets exactly, each triangular facet would need to be different. Fortunately, a triangular facet can be rotated so that the direction of the toroid is within 30° of the ideal direction of the parabola. This enables the use of identical, interchangeable toroidal facets for a group of facets.

The positioning of four groups of toroidal facets on the offset collector is shown in figure 16. The four groups are differentiated by 1, 2, 3, or 4 crosshatch lines through each triangular facet. The direction of the longest radius of curvature of the toroid is along the crosshatch lines. Note that groups 2 and 4 have the longest radius of curvature parallel to one side of the triangle and the other groups have the longest radius of curvature perpendicular to one side. The preferred facet orientation is to have the longest radius of curvature radially outward from the parabolic axis. Note, that some of the facets in figure 16 are in different groups than the facets in figure 2 to better line up with the radial direction. Radii of curvature for the four groups of toroidal facets are listed below.

Group Number:	1	2	3	4
Radius along lines, cm:	1963	2438	3038	3830
Radius across lines, cm:	1844	1996	2154	2314

One triangular facet on each hexagonal panel in figure 16 has a heavy outline. The ideal images (assuming a point light source and no slope errors) of these toroidal facets are shown passing through the receiver aperture in figure 17(a). Corresponding ideal images for spherical facets are shown in figure 17(b). These spherical facet images shown on figure 17(b) are an enlarged view of the facet images passing through the aperture on figure 9. The images of the toroidal facets (fig. 17(a)) are much smaller than the images of the spherical facets (fig. 17(b)), because the toroidal facets are a much better match to the exact parabolic contour.

Spreading due to slope errors as shown in figure 8 and to the size of the solar image as shown in figure 6, will enlarge these ideal images in figure 17

and cause power to be lost by interception with the aperture plate. These intercept losses for parabolic, toroidal, and spherical facets having 3 mrad slope error are shown as a function of aperture radius in figure 18. The losses for toroidal facets are significantly less than for spherical facets. They are almost as low as for parabolic facets, although there are only four groups of toroidal facets, but each of the 456 parabolic facets would require a different contour.

CONCLUSIONS

A ray tracing computer code is being developed by NASA Lewis to study the offset collector for the space station solar dynamic electric power system. This code traces rays from 50 points on the Sun to 10 points on each of 456 triangular facets. The rays are reflected, accounting for facet contour and slope error, then traced through the receiver aperture to the walls of the receiver.

Light patterns representing images of the Sun and images of the collector and its facets on the walls of the receiver are computed. The size of the images of the Sun varies by about a factor of three due to variations in the angles of intersection of the rays with the receiver walls and variations of distance from different points on the collector to the receiver walls. Rays from the center of the Sun reflected by the edges of ideal parabolic facets produce an image of the collector inside the receiver. Surface slope errors of 1 mrad move the nodal points to new locations relative to the ideal facet images. Larger distortions and in some cases severe elongation of facet images result from spherically contoured facets.

Output from the OFFSET code is in good agreement with corresponding output from MDAC's DPAP code and GTRI's OPTIC code. Moving the receiver aperture to the edge rather than the center of the receiver aperture plate was found to improve the receiver flux distribution. A major reduction of aperture intercept power loss was found to be possible by using toroidal facets instead of spherical facets. The performance with toroidal facets is almost as good as with the ideal parabolic contour, although only four groups of identical, interchangeable, toroidal facets are required.

REFERENCES

1. Elfe, T., 1982, "Modeling High Temperature Solar Receivers" Proceedings of Solar Thermal test Facility User's Association Workshop on High Temperature Materials for Solar Thermal Applications.

2. Blackmon, J.B., Cross C.R., Hennen, D.E., McFee, R.H., Goswami, D.Y., Watauabe, K., and Healey, H.M., 1987, "Design and Performance of a Digital Image Radiometer for Dish Concentrator Evaluation" Solar Engineering 1987, D.Y. Goswami, K. Watanabe, and H.M. Healy, eds., American Society of Mechanical Engineering, New York, Vol. 1, pp. 318-323.

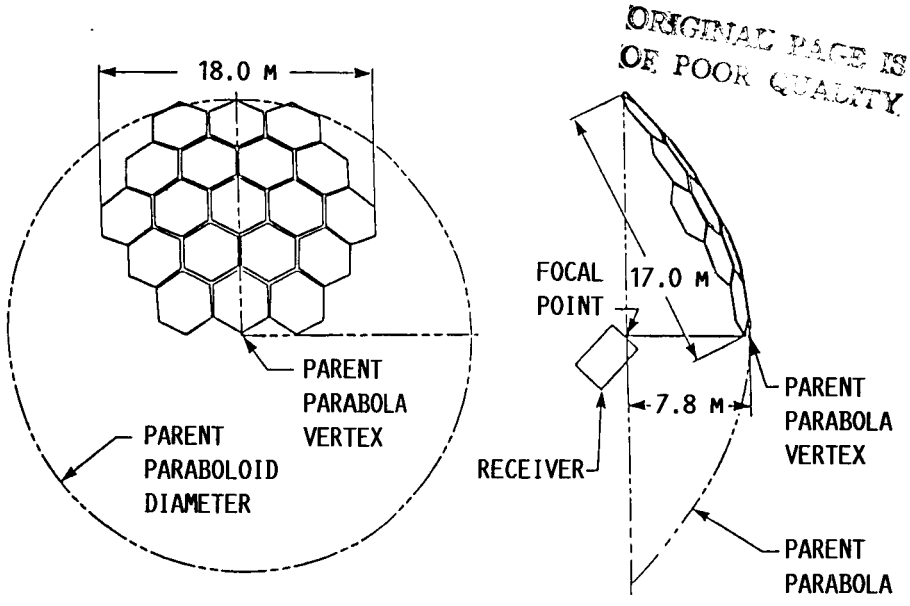

FIGURE 1. - OFFSET NEWTONIAN COLLECTOR GEOMETRY.

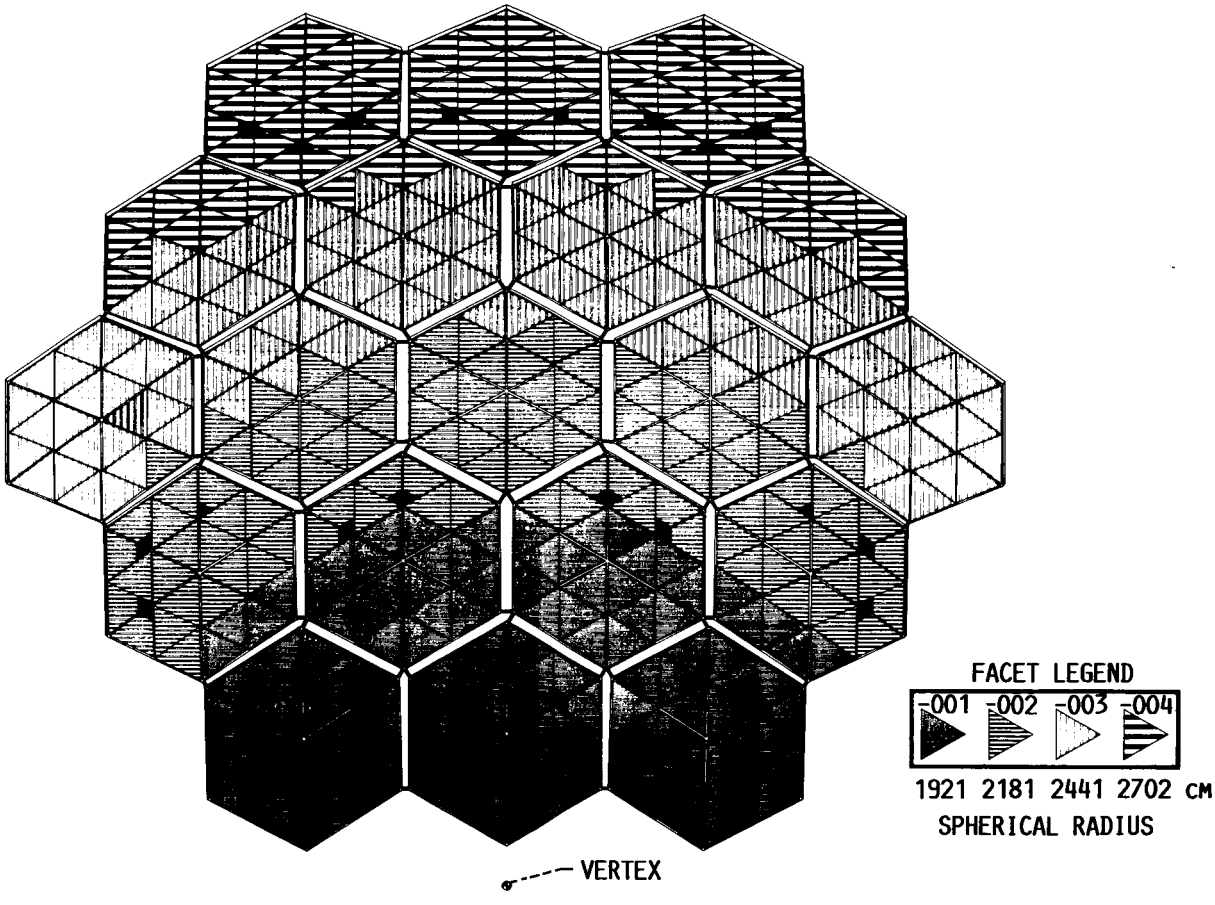

FIGURE 2. - OFFSET COLLECTOR.

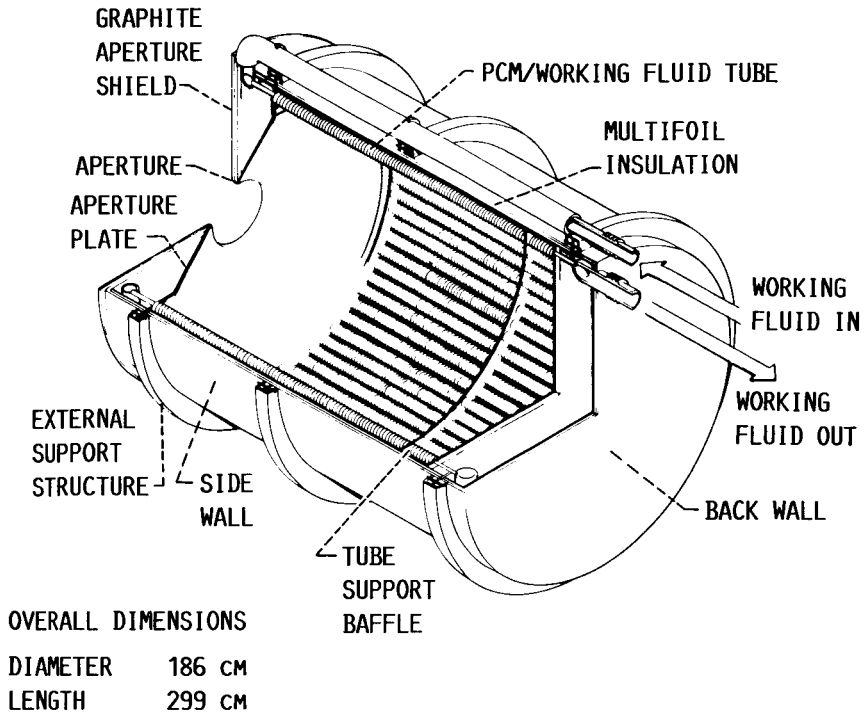

FIGURE 3. - SPACE STATION RECEIVER.

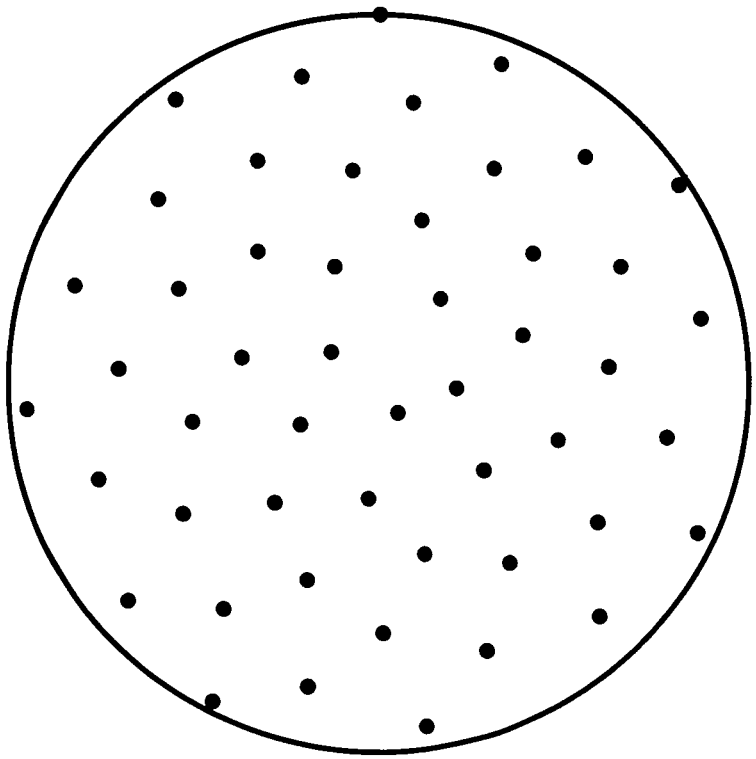

FIGURE 4. - LOCATIONS OF 50 RAY SOURCES ON THE SUN.

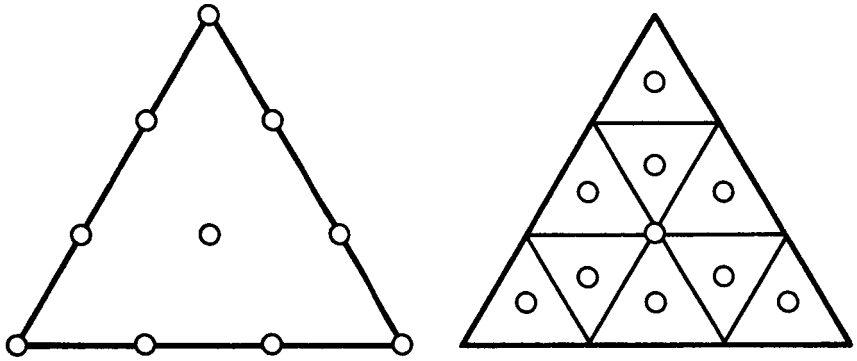

(A) FACET IMAGING. (B) FLUX DISTRIBUTIONS.

FIGURE 5. - TEN NODEL POINTS ON EACH FACET.

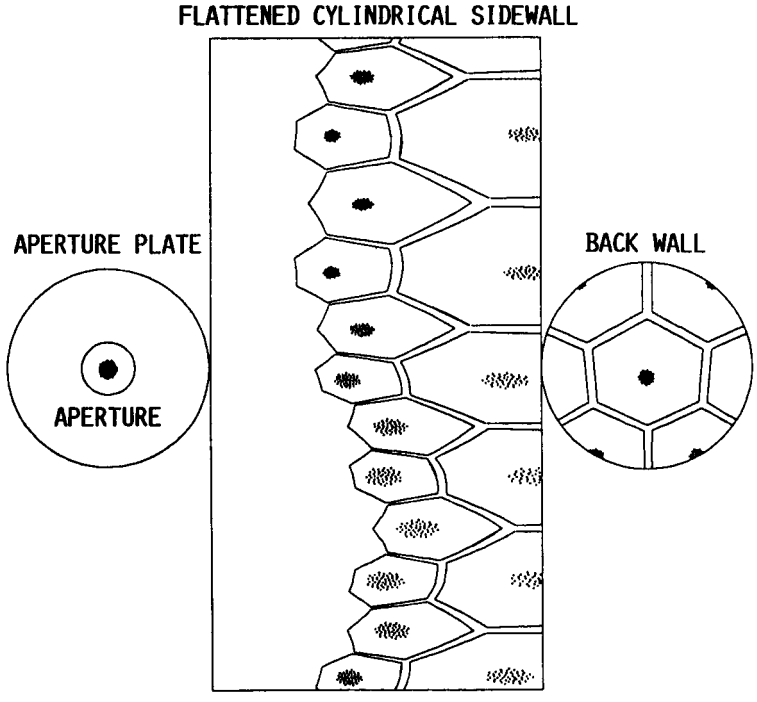

FIGURE 6. - IMAGES OF THE SUN FROM THE CENTERS OF 19 HEXAGONAL PANELS.

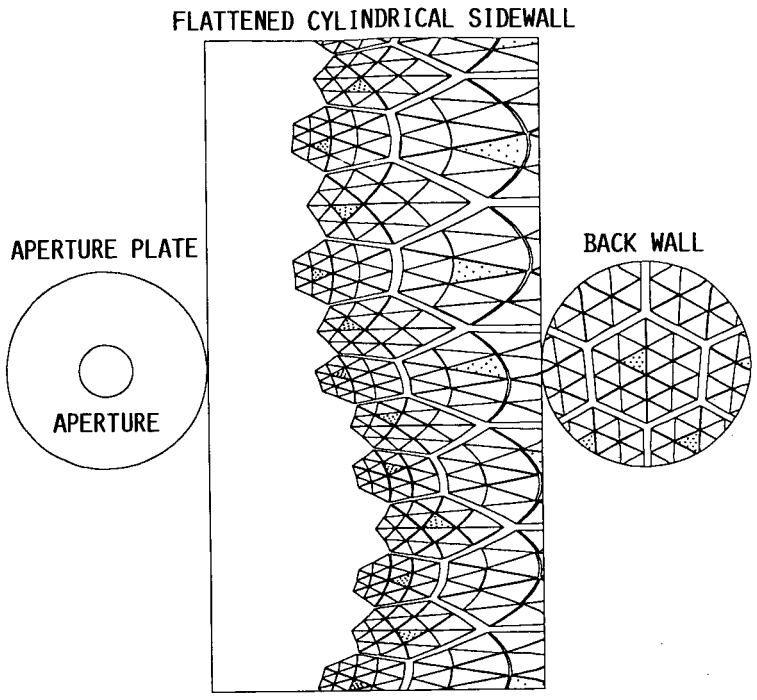

FIGURE 7. - IMAGE OF AN IDEAL COLLECTOR PRODUCED BY RAYS FROM THE CENTER OF THE SUN.

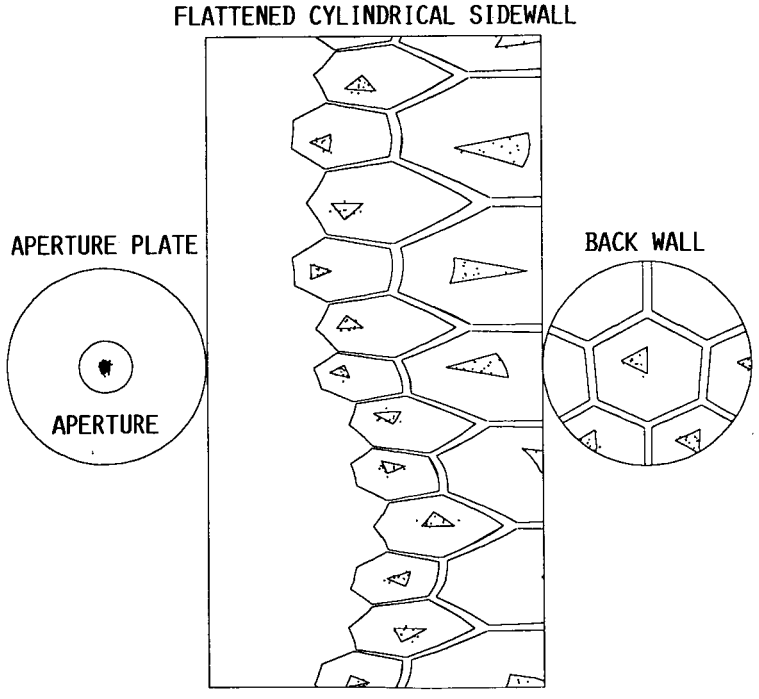

FIGURE 8. - IMAGES OF SELECTED PARABOLIC CONTOUR FACETS AND OF NODAL POINTS WITH ONE MILLIRADIAN SLOPE ERROR.

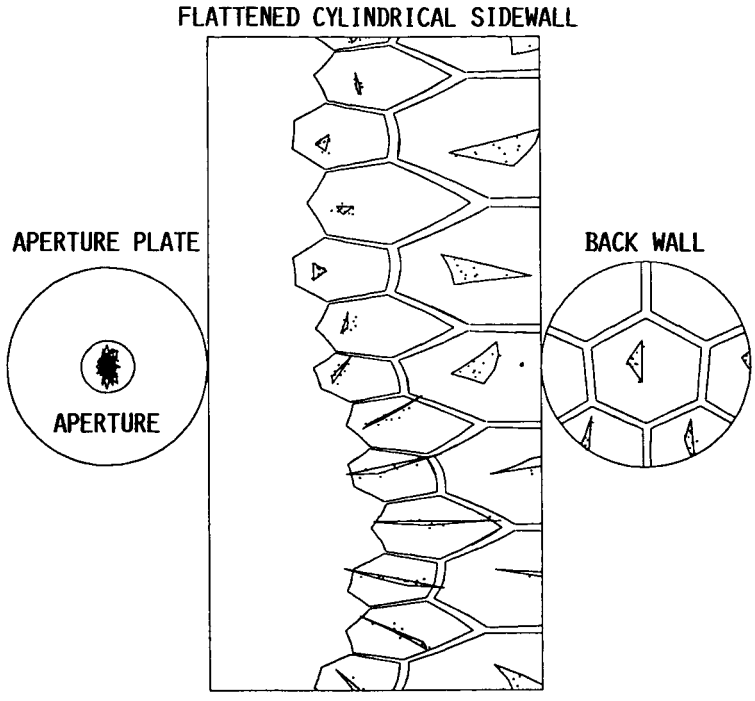

FIGURE 9. - IMAGES OF SELECTED SPHERICALLY CONTOURED FACETS AND OF NODAL POINTS WITH ONE MILLIRADIAN SLOPE ERROR.

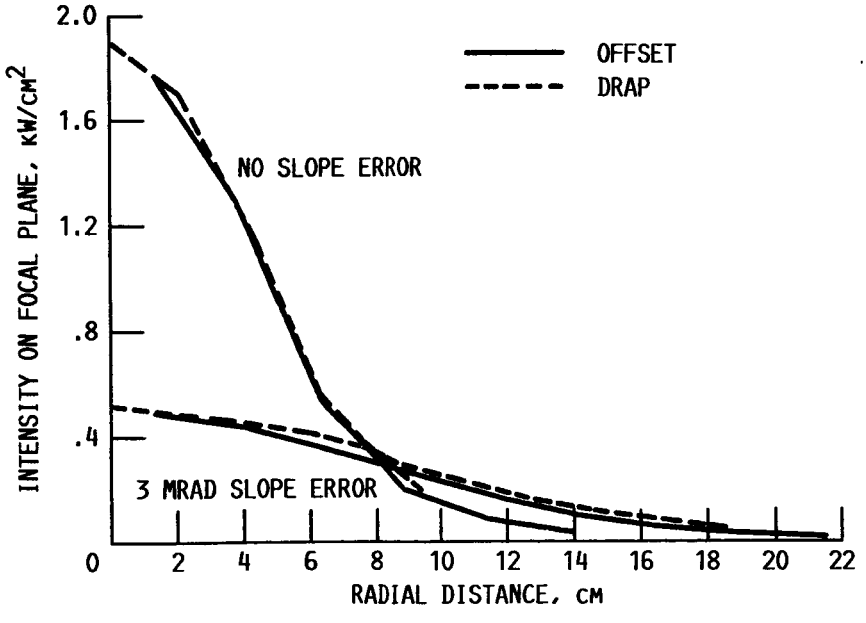

FIGURE 10. - FOCAL PLANE INTENSITY COMPARISON OF DRAP AND OFFSET CODES.

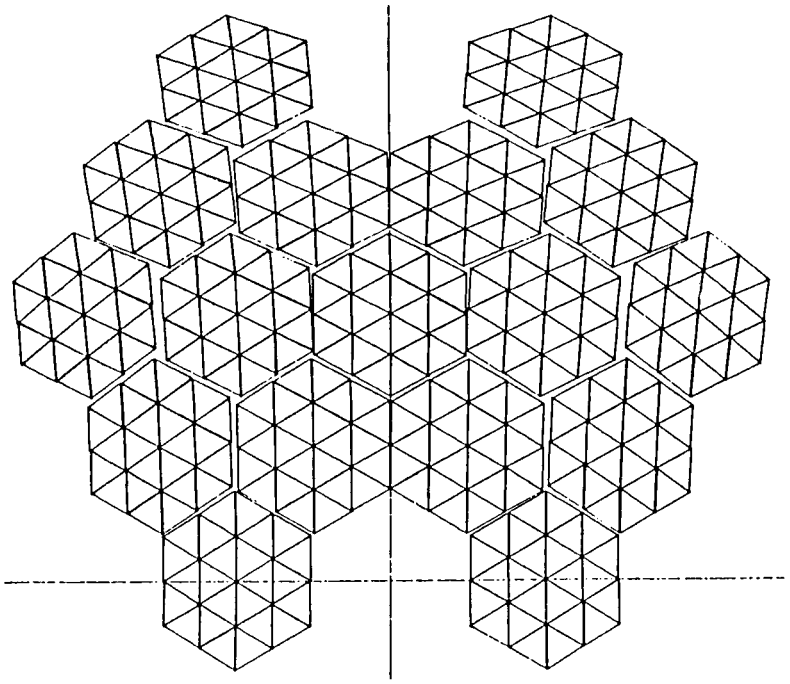

FIGURE 11. - BRAYTON OFFSET COLLECTOR. ORIGINAL CONFIGURATION.

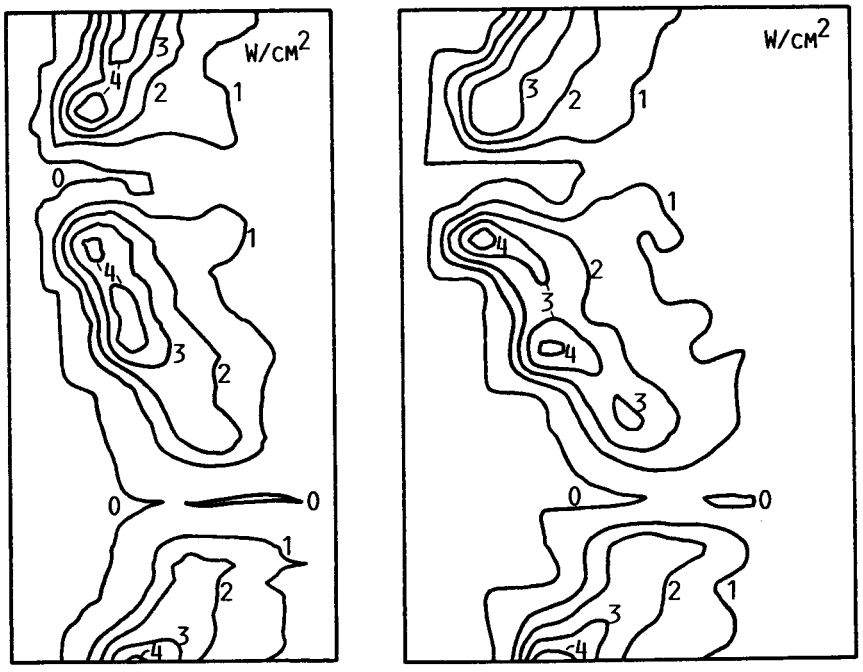

(A) NASA OFFSET CODE. (B) GTRI OPTIC CODE.

FIGURE 12. - RECEIVER SIDEWALL FLUX COMPARISON.

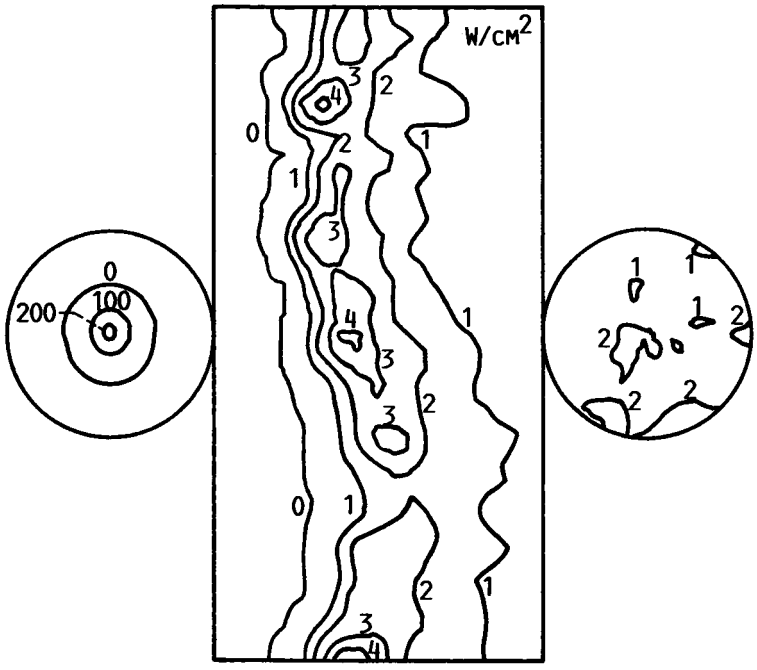

FIGURE 13. - RECEIVER FLUX MAP FROM 19 PANEL COLLECTOR.

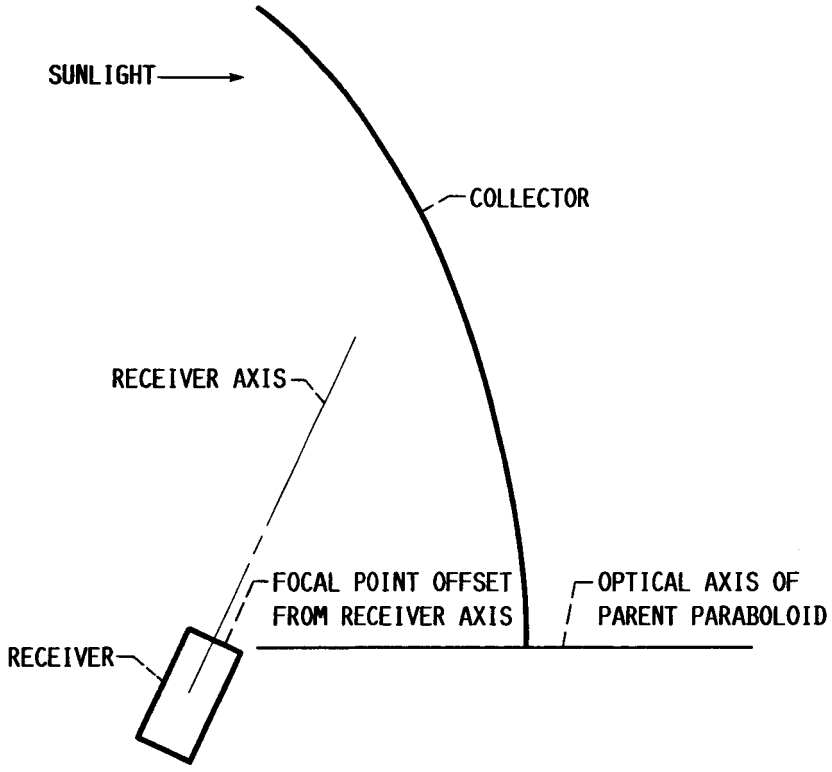

FIGURE 14. - REVISED CONFIGURATION WITH OFFSET RECEIVER APERTURE AND INCREASED RECEIVER TILT.

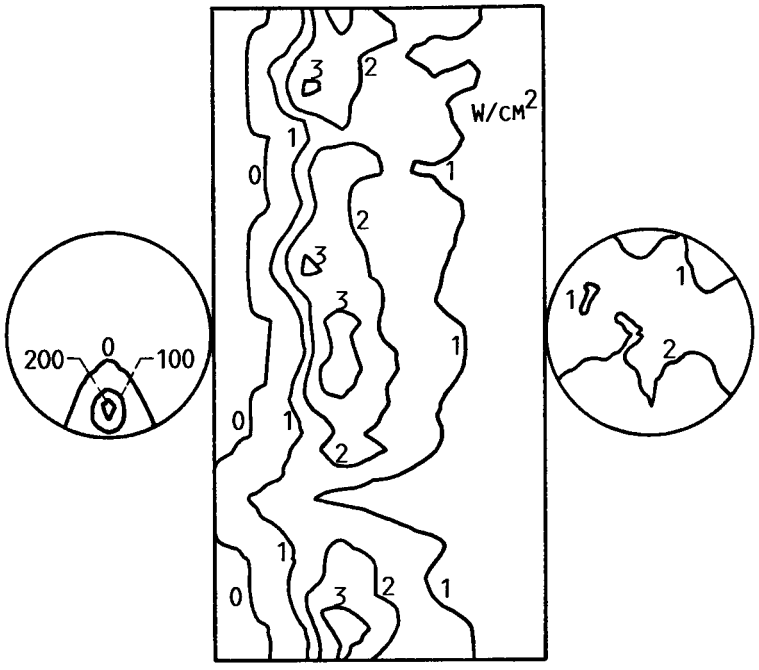

FIGURE 15. - RECEIVER FLUX MAP FROM REVISED CONFIGURATION.

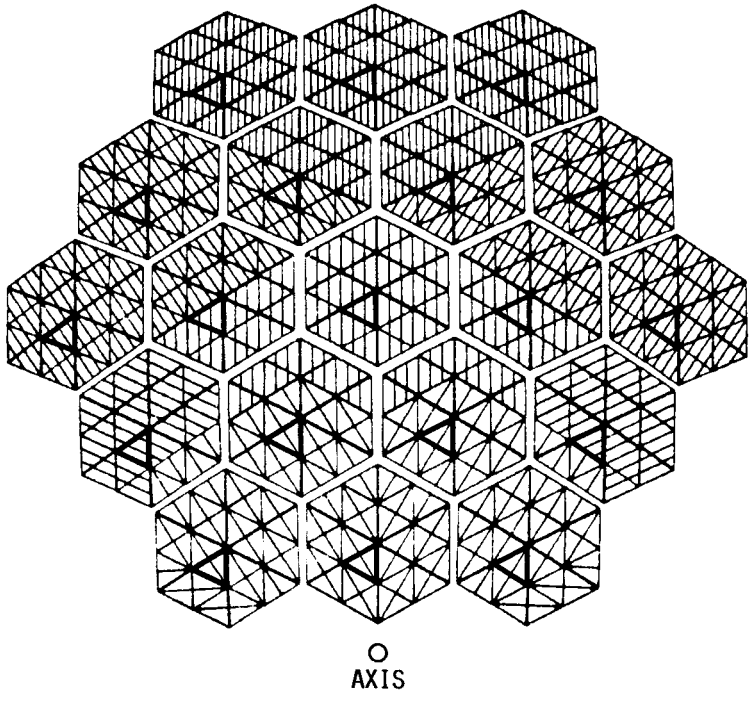

FIGURE 16. - OFFSET COLLECTOR WITH FOUR GROUPS OF TOROIDAL FACETS.

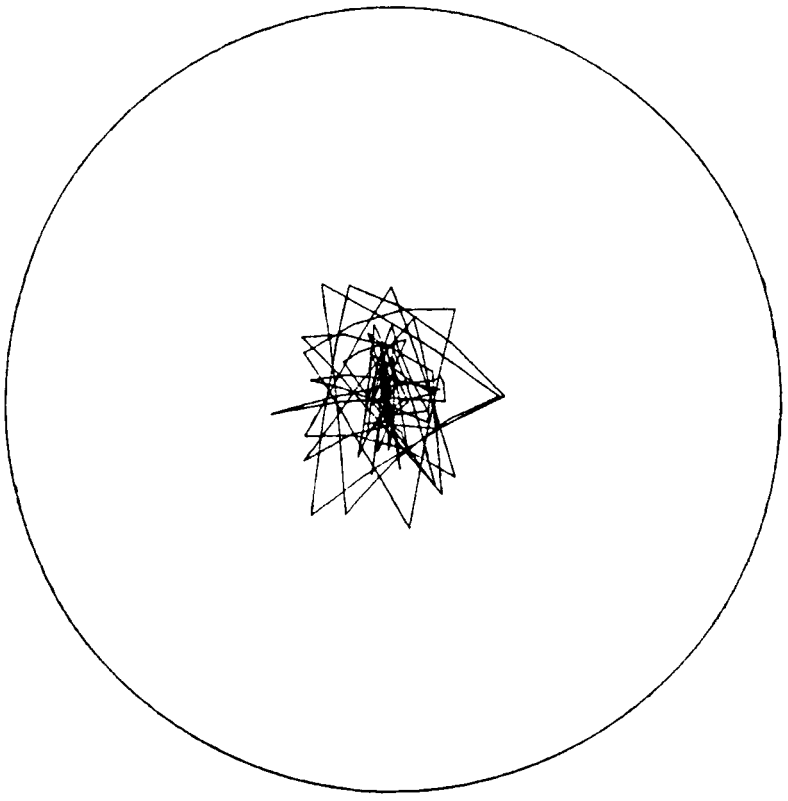

(A) TOROIDAL FACETS.

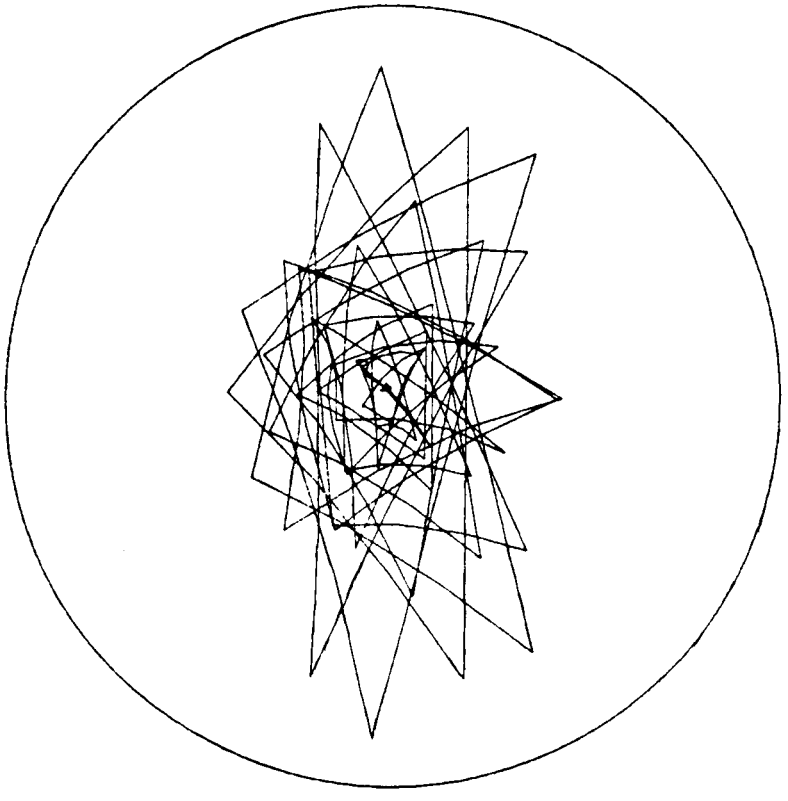

(B) SPHERICAL FACETS.

FIGURE 17. - RECEIVER APERTURE IMAGES OF COLLECTOR FACETS.

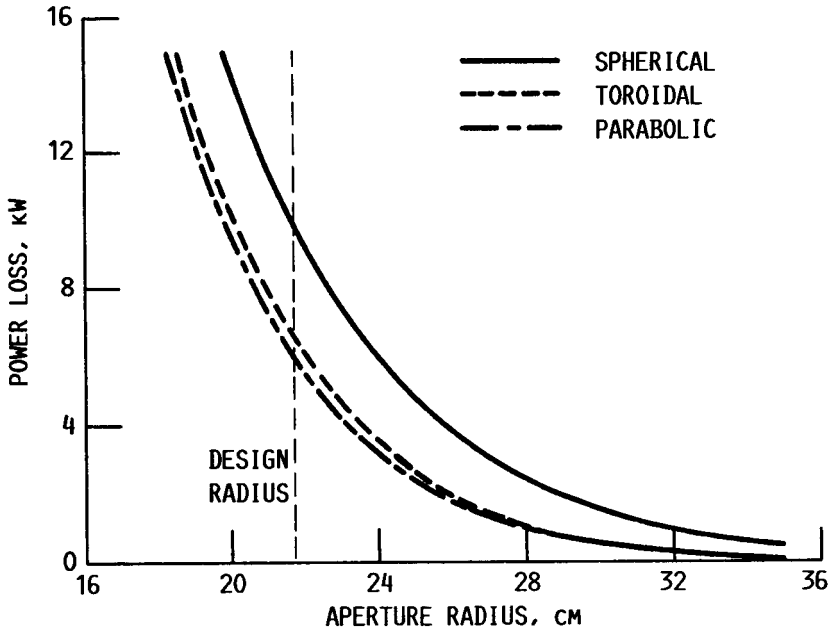

FIGURE 18. - APERTURE INTERCEPT POWER LOSS WITH DIFFERENT FACET CONTOURS.

NASA
National Aeronautics and Space Administration

Report Documentation Page

1. Report No.	2. Government Accession No.	3. Recipient's Catalog No.
NASA TM-100853		

4. Title and Subtitle
Ray Tracing Optical Analysis of Offset Solar Collector for Space Station Solar Dynamic System

5. Report Date

6. Performing Organization Code

7. Author(s)
Kent S. Jefferies

8. Performing Organization Report No.
E-4056

10. Work Unit No.
474-12-10

9. Performing Organization Name and Address
National Aeronautics and Space Administration
Lewis Research Center
Cleveland, Ohio 44135-3191

11. Contract or Grant No.

13. Type of Report and Period Covered
Technical Memorandum

12. Sponsoring Agency Name and Address
National Aeronautics and Space Administration
Washington, D.C. 20546-0001

14. Sponsoring Agency Code

15. Supplementary Notes
Prepared for the 23rd Intersociety Energy Conversion Engineering Conference cosponsored by the ASME, AIAA, ANS, SAE, IEEE, ACS, and AIChE, Denver, Colorado, July 31 - August 5, 1988.

16. Abstract
OFFSET, a detailed ray tracing computer code, was developed at NASA Lewis Research Center to model the offset solar collector for the Space Station solar dynamic electric power system. This model traces rays from 50 points on the face of the Sun to 10 points on each of 456 collector facets. The triangular facets are modeled with spherical, parabolic, or toroidal reflective surface contour and surface slope errors. The rays are then traced through the receiver aperture to the walls of the receiver. Images of the collector and of the Sun within the receiver produced by this code provide insight into the collector receiver interface. Flux distribution on the receiver walls, plotted by this code, is improved by a combination of changes to aperture location and receiver tilt angle. Power loss by spillage at the receiver aperture is computed and is considerably reduced by using toroidal facets.

17. Key Words (Suggested by Author(s))
Solar collector; Solar concentrator; Mathmatical model; Solar dynamic power

18. Distribution Statement
Unclassified - Unlimited
Subject Category 20

19. Security Classif. (of this report)	20. Security Classif. (of this page)	21. No of pages	22. Price*
Unclassified	Unclassified	20	A02

*For sale by the National Technical Information Service, Springfield, Virginia 22161